

Alternative computational methods for Boltzmann and Wigner models in charged transport systems

Irene M. Gamba

Department of Mathematics and ICES, The University of Texas at Austin
201 East 24th St, Stop C0200, Austin, Texas 78712-1229, USA. e-mail: gamba@math.utexas.edu

Abstract—We will discuss recent development in the simulation of Boltzmann-Poisson systems and Wigner transport by deterministic numerical solvers. We have proposed to solve linear transport problems using a Discontinuous Galerkin (DG) Finite Element Method (FEM) approach that allows adaptivity and accuracy by a flexible choice of basis functions, as well as numerical efficiency by parallelization and scalability. In the case of non-linear transport, spectral methods may be competitive for the calculation of anisotropic scattering. Such numerical schemes can be competitive to DSMC methods and have the advantage of an easy and accurate implementation of boundary conditions including charge neutrality at contacts and specular and diffusive reflection at insulating and interface boundaries. These deterministic solvers are able to resolve small scales (or order 10^{-7} to 10^{-6}) that DSMC approach may not be able to handle

THE BOLTZMANN-POISSON (BP) MODEL

The dynamics of hot electron transport in modern semiconductor devices can be described by the semiclassical (BP) model

$$\frac{\partial f_i}{\partial t} + \frac{1}{\hbar} \nabla_k \varepsilon_i \cdot \nabla_x f_i - \frac{q_i}{\hbar} E \cdot \nabla_k f_i = \sum_j Q_{i,j}(f_i, f_j)$$

$$\nabla_x \cdot (\epsilon \nabla_x V) = \sum_i q_i \rho_i - N(x), E = -\nabla V$$

where $f_i(x, k, t)$ is the probability density function (pdf) over phase space (x, k) of a carrier in the i -th energy band in position x , with crystal momentum $\hbar k$ at time t . The collision operators $Q_{i,j}(f_i, f_j)$ model i -th and j -th carrier recombinations, collisions with phonons or generation effects. $E(x, t)$ is the electric field, $\varepsilon_i(k)$ is the i -th energy band surface, the i -th charge density $\rho_i(t, x)$ is the k -average of f_i , and $N(x)$ is the doping profile. The collision operator $Q_{i,j}(f_i, f_j)$ describes electron-phonon interactions where most important ones in Si are due to scattering with lattice vibrations of the crystal, modeled by acoustic and optical non-polar modes with a single frequency ω_p , whose intra band transition probability rates are given by the Fermi Golden Rule and are proportional the phonon occupation factor $[\exp(\frac{\hbar\omega_p}{k_B T_L}) - 1]^{-1}$ where k_B is the Boltzmann constant and $T_L = 300^\circ K$ is the constant lattice temperature.

This kinetic system is posed in six dimensions plus time for a full 3-D device model. Traditionally, this high dimensional system has been a motivation to be solved by the stochastic

Direct Simulation Monte Carlo (DSMC) methods. Yet, we proposed in [2] a novel deterministic approach based Discontinuous Galerkin (DG) Finite Element Method (FEM) for solving the Boltzmann-Poisson system that can be very competitive for hot electron transport calculations. The DG approach is suitable for strong transport conditions and is very adaptable and locally accurate due to flexible choices of basis functions. It is also very suitable for scalability and parallelization as well as efficient for full band transport by coupling the BP with Pseudo Empirical Methods for crystallographic calculations [1], [9] as band anisotropy far away from the local conduction band minimum, as it is needed for a correct description of the energy band and related group velocity for the charge carriers in hot electronic transport. Detailed description of DG methods and examples of applications of the DG scheme to 1D diode and 2D double gate MOSFET devices can be found in this references. We just mention in Figure a couple of plots of the steady surfaces for the pdf $f(x, k, t)$ solution of the (BP) system in 2- \mathbf{x} space, and 3- \mathbf{k} -wave space simulation of a double gate MOSFET of a 150nm length and 10nm thickness and a 50nm effective channel.

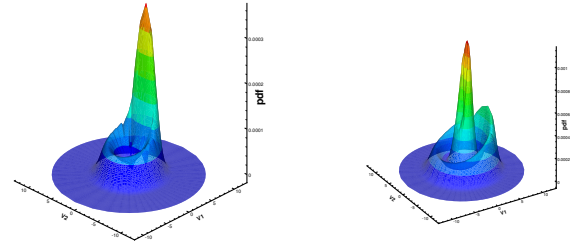


Fig. 1. pdf of a single electron carrier for the BP system model for a 2D double gate MOSFET at $t = 0.5$, $(x, y) = (0.09375, 0.10)$ (left) and $(x, y) = (0.125, 0.12)$ (right).

A new focus is the study of boundary conditions effects for BP transport. These conditions vary according to device physics and geometry and they are mainly contact, insulating and interface conditions. Charge neutrality conditions are impose at contacts: $f_{out}(t, \vec{x}, \vec{k})|_{\Gamma} = N_D(\vec{x}) \frac{f_{in}(t, \vec{x}, \vec{k})|_{\Gamma}}{\rho(t, \vec{x})}$, Γ subset of $\partial\Omega_{\vec{x}}$.

Insulating reflecting boundaries conditions at the kinetic level are also well defined by

$$f(\vec{x}, \vec{k}, t) = \alpha(k) f(\vec{x}, \vec{k}', t) + (1 - \alpha(k)) C e^{-\varepsilon(\vec{k})/K_B T}$$

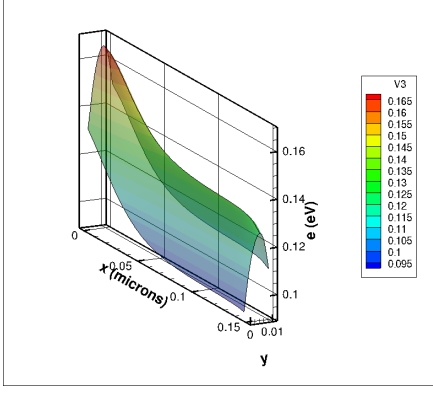


Fig. 2. Mean energy e (eV) vs. Position (x, y) in (μm) plot for Mixed specular-diffusive reflection condition with accommodation coefficient $\alpha(k)$ with $l_r = 0.5$ and 1.0 eV bias

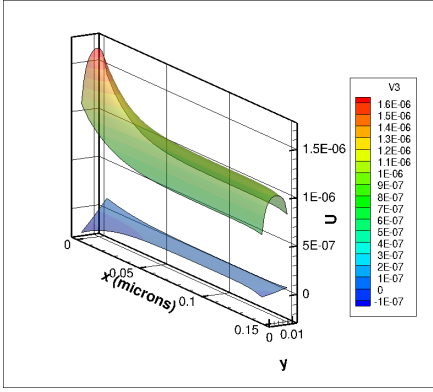


Fig. 3. Momentum $U(10^{28} \frac{cm^{-2}}{s})$ vs. Position (x, y) in (μm) for plot for Mixed specular-diffusive reflection condition with accommodation coefficient $\alpha(k)$ with $l_r = 0.5$ and 1.0 eV bias

$$\int_{\nabla_{\vec{k}} \varepsilon \cdot \eta > 0} \nabla_{\vec{k}} \varepsilon \cdot \eta(\vec{x}) f d\vec{k}$$

for $(\vec{x}, \vec{k}) \in \Gamma_N^-$, $t > 0$ such that $\nabla_{\vec{k}} \varepsilon(\vec{k}') = \nabla_{\vec{k}} \varepsilon(\vec{k}) - 2(\nabla_{\vec{k}} \varepsilon(\vec{k}) \cdot \eta(\vec{x}))\eta(\vec{x})$ [4], [10], [11].

They represent a convex combination of specular and diffusive reflection conditions, where the *accommodation coefficient* $\alpha(k)$ is a probability density representing the percentage of specularity that carries information of boundary variations. See [7] for a sketch of the DG implementation of mixed specular and diffusive reflection conditions implemented for the Boltzmann-Poisson system of electron transport in bulk with Kane dispersion energy band. The choice of the probability density is $\alpha(k) = e^{-4L_r^2|k|^2 \cos^2 \Theta} = \exp(-4l_r^2 w(1 + a_k w) \sin^2 \varphi) = p(w, \varphi)$, as a Gaussian distribution depending on k written in terms of band energy coordinates and a parameter l_r being the (normalized) *rms* rough interface height. When these variations are strong boundary layer formation may be expected [5], [8], [10].

THE WIGNER-FOKKER-PLANCK (WFP) MODEL

As a further application of the DG-FEM scheme, we also proposed the study by this approach of the following simple

benchmark problem, for the quasi-classical transport model for the evolution of a single electron wave function driven by a potential $V(x)$,

$$\frac{\partial w}{\partial t} + \nabla_k \varepsilon \cdot \nabla_x w + \Theta_{\hbar}[V](w) = Q_{\hbar, FP}(w)$$

where the function $w(x, k, t)$ is the *Wigner transform* of the density matrix $\rho(x, y, t)$, and [12]. is understood as a quasi-probability function, which may take on negative values. The nonlocal pseudo-differential operator $\Theta[V]$, acting on the potential V , is defined by

$$\begin{aligned} \Theta[V](w) &= - \int \frac{i\delta_{\hbar} V(x, \eta)}{\hbar (2\pi)^d} w(x, k') e^{i\eta \cdot (k-k')} dk' d\eta, \\ &= -\Im (\mathcal{F}^{-1} [\delta V](x, \cdot)) * w(x, \cdot, t), \end{aligned}$$

$$\text{with } \delta_{\hbar} V(x, \eta) = V(x + \frac{\hbar}{m} \frac{\eta}{2}) - V(x - \frac{\hbar}{m} \frac{\eta}{2}).$$

This operator is a strongly dispersive one, except for the harmonic potential, since $\Theta[\frac{|v|^2}{2}](w) = q x \cdot \nabla_k w$ yields classical particle transport dynamics. A performance boost is possible for finite sinusoidal approximation to the potential: This dispersive form produces a series of Dirac δ -distributions that can be easily computed by immediate integration. In particular any linear combination of potentials is easily implemented (i.e FFT for potentials).

The right hand side models the averaged environmental interactions with the system and is referred to as the Quantum Fokker-Planck operator

$$\begin{aligned} Q_{\hbar, FP}(w) &= D_{qq} \Delta_x w + 2\gamma \nabla_k k w \\ &+ 2 \frac{D_{pq}}{m} \text{div}_x (\nabla_k w) + \frac{D_{pp}}{m^2} \Delta_k w \end{aligned}$$

which is derived from a heat bath of harmonic oscillators, where T is its temperature, λ the coupling constant, and Ω the cut-off frequency. The coefficients $D_{i,j}$, for $i, j \in \{p, q\}$ depend on the scaled Plank constant \hbar , particle mass m , and the Boltzmann's constant k_B as well as on λ , Ω . In addition they satisfy the Lindblad condition:

$$D_{qq} D_{pp} - D_{pq}^2 \geq \hbar^2 \lambda (2m)^{-2} / 4,$$

or equivalently $\Omega \leq k_b T / \hbar$, [6]. These conditions recover the quantum mechanically correct evolution of the system, and convergence to classical Fokker-Planck dynamics from stochastics as $\hbar \rightarrow 0$.

The DG-FEM method for the WFP equation was developed in [3] along with analytic stability and convergence estimates, as well as numerical experiments and simulations. The scheme performs very accurately on coarse meshes by using dressed basis functions for bounded perturbations of the harmonic potential $V(x) = |x|^2/2$. This strategy consists in weighting the basis functions by either, for example, Hermite functions or better performing weights are *quantum Maxwellian* stationary state of the WFP model for the harmonic potential $V(x)$. The challenge lies in the implementation of a suitable method for the pseudo-differential operator, $\Theta(V)(w)$. One case easily see that sinusoidal approximations may be the more efficient.

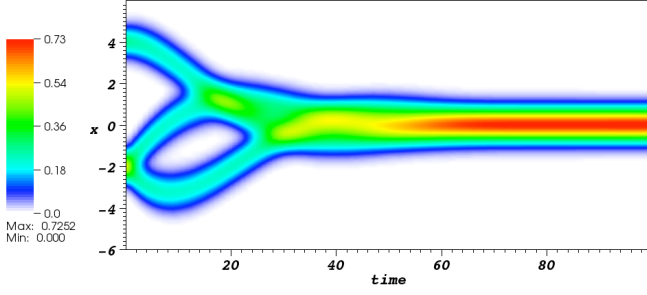


Fig. 4. Density plot of the convergence of a three centered initial state to the unique steady state of WFP equation with a harmonic potential. The numerical solution is essentially zero in the white regions.

The main challenge was to produce an accurate and practical treatment of the highly dispersive pseudo-differential term. The proposed method do this in a manner that falls neatly into the DG formalism, and a wide range of potential functions may be treated. Linear combinations of harmonic, sinusoidal, and step functions were demonstrated, and it is clear how to apply the method to Gaussian and other families of potential functions.

Numerical benchmarks: The DG scheme was implemented in one dimensional domains in (x, k) -space, partitioned into a regular rectangular mesh. To verify the numerical implementation, several tests were conducted using various potentials and different approximation spaces. We chose $\hbar = m = 1$ and $\Omega = 0$.

Harmonic potential - Single well: $V(x) = \frac{x^2}{2}$. For this choice of potential the Wigner evolution is classical, and so the initial states evolves spiraling toward a unique steady state, independent of the initial data. We set an initial state of three displaced Maxwellians, averaged to unity: $w_I = \frac{2}{3\pi} \{ \exp[-2((x-4)^2 + (k^2))] + \exp[-2(x+2)^2] \exp[-(k-2\sqrt{3})^2] + \exp[-(k+2\sqrt{3})^2] \}$. The convergence to the steady state is depicted in Figure 4, a plot of charge density, $\rho(x, t) = \int w(x, k, t) dk$. Since density is a projection of the solution onto space (x, t) , w_I initially appears to have only two centers due to a symmetry, which is immediately broken as the three centers spiral around the origin, exhibiting the classical dynamics behavior.

Periodic perturbation - Triple Well Finally, the dispersive behavior can be clearly seen when the DG method is used to calculate the behavior of an initial Maxwellian in a periodically perturbed confining potential. The potential used was $V(x) = \frac{x^2}{2} + 30(1 - \cos(x))$.

The potential is pictured in the inset in the upper Figure 6. It has three deep wells, at the origin and near $\pm 2\pi$. The initial state was a Maxwellian concentrated about a large positive value of x and negative value of k to give it a rapid initial motion toward the origin. A projection of the initial state onto the x axis is also provided in the inset to Figure 6 (its width has been exaggerated for the purpose of illustration). During the course of the simulation, the center of mass (charge) flows

down the potential wall, and a short way up the other side before becoming concentrated in two of the wells. The total mass is preserved to within 10^{-5} during the simulation. The time-step was $dt = 0.001$, $\Omega = [-20, 30] \times [-35, 15]$, and the mesh measured 200×200 . At any given time, the total mass contained outside the 0.005 contour level (the white area) is essentially zero. The vertical lines at $t = 33, 37, 41$, and 45 correspond the snapshots of the solution shown below. The frame at $t = 33$ represents a moment when the solution is spilling over from the well at $x \approx -2\pi$ into the well at the origin. The remaining frames show each part of the solution completing a circuit of its respective well. As indicated by Figure 6, the solution settles into these wells and in each case takes on an appearance very similar to a pair of Maxwellian.

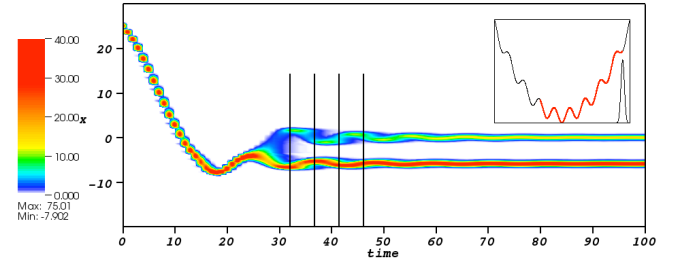
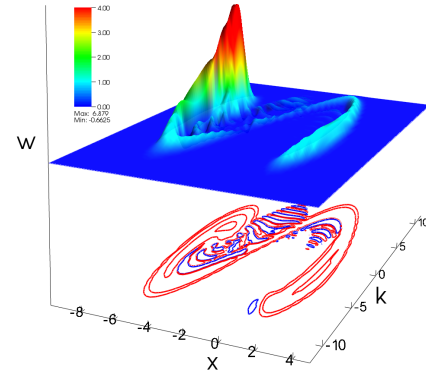


Fig. 5. A plot of the DG computed Wigner charge density $\rho(x, t) = \int w(x, k, t) dk$ with piecewise linear basis functions. The inset shows the potential, and a projection of the initial state. The numerical solution settles into two of the three deep wells of this potential at $x = 0$ and $x \approx -2\pi$. The four vertical lines indicate the times $t = 33, t = 37$ (middle, left and right); and $t = 41, t = 45$.



ACKNOWLEDGMENT

The author have been partially funded by NSF grants CHE-0934450, DMS-1109625, and DMS-RNMS-1107465.

REFERENCES

- [1] J. Chelikowsky, and M. Cohen, *Electronic Structure of Silicon*, Physical Review B **10**, 12 (1974).
- [2] Y. Cheng, I. M. Gamba, A. Majorana, and C.W. Shu, *A Discontinuous Galerkin solver for Boltzmann-Poisson systems in nano-devices*, CMAME **198**, 3130-3150 (2009).

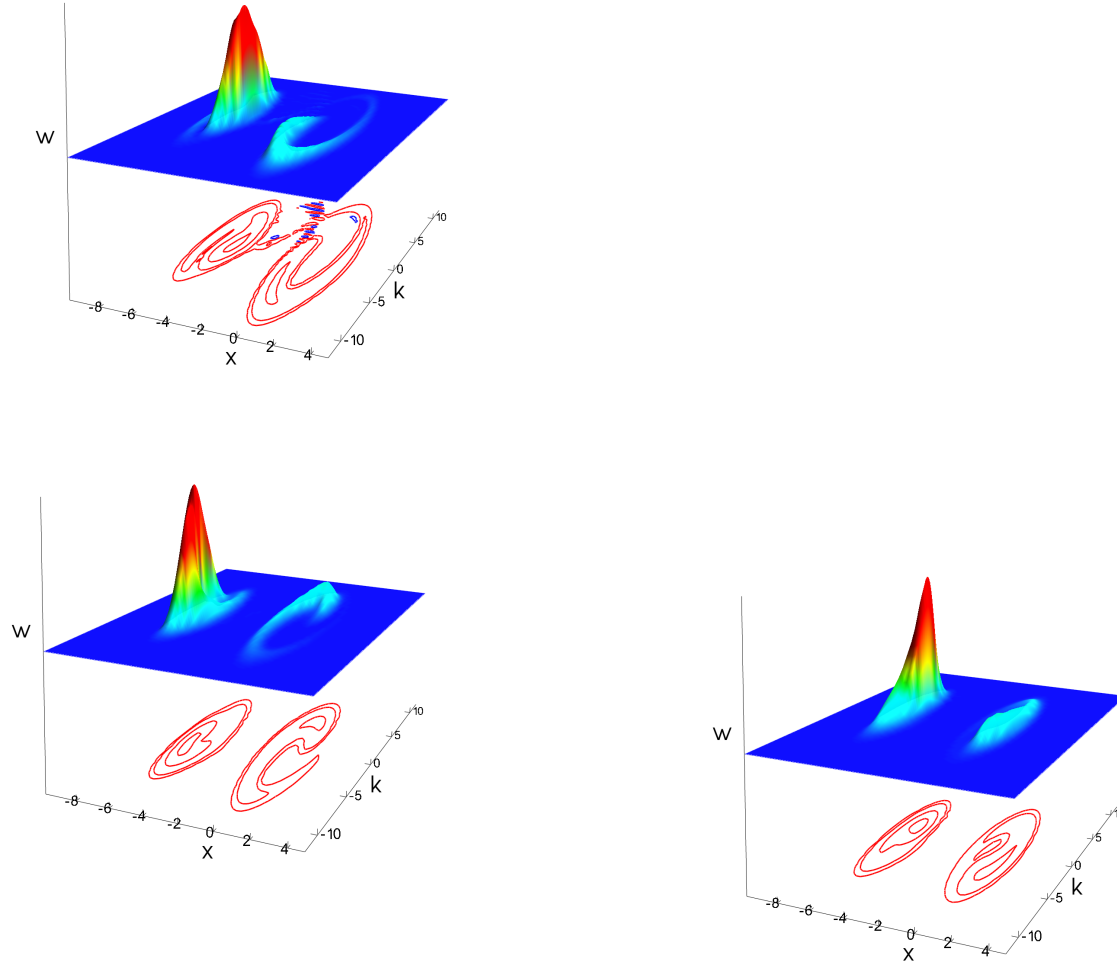


Fig. 6. The numerical solution settles into two of the three deep wells of this potential at $x = 0$ and $x \approx -2\pi$. The four vertical lines indicate the times $t = 33, t = 37, t = 41$ and $t = 45$, from top to bottom respectively, where the Wigner solution $w(x, k, t)$ frames completing a circuit of these two wells.

- [3] I.M. Gamba, M.P. Gualdani and R. Sharp, *An Adaptable Discontinuous Galerkin Scheme for the Wigner-Fokker-Planck Equation*, Commun. Math. Sci. Vol. 7, No. 3 pp. 635-664 (2009).
- [4] A. Jungel, *Transport Equations for Semiconductors*, Springer Verlag (2009).
- [5] Z. Aksamija, I. Knezevic, *Thermal conductivity of $Si_{1-x}Ge_x/Si_{1-y}Ge_y$ superlattices: Competition between interfacial and internal scattering* Phys.Rev. B **88**, (2013).
- [6] G. Lindblad, *On the generators of quantum mechanical semigroups*, Comm. Math. Physics **48**, 119130 (1976).
- [7] J.A. Morales Escalante and I.M. Gamba, *Boundary conditions effects by Discontinuous Galerkin Solvers for Boltzmann-Poisson models of Electron Transport*, IEEE Xplore, 2014 International Workshop on Computational Electronics (IWCE), June 2015.
- [8] J.A. Morales Escalante and I.M. Gamba, *Discontinuous Galerkin schemes for diffusive reflection for Boltzmann-Poisson electron transport with rough boundaries*, in preparation (2014).
- [9] J.A. Morales Escalante, I.M. Gamba, A. Majorana, Y. Cheng, C.-W. Shu, and J.R. Chelikowsky, *Deterministic DG Solvers for EPM-Boltzmann-Poisson Transport*, IWCE16 Abstracts, 2013.
- [10] Y. Sone, *Molecular Gas Dynamics: Theory, Techniques, and Applications*, Birkhauser (2007).
- [11] S. Soffer *Statistical Model for the size effect in Electrical Conduction*, Journal of Applied Physics 38 1710 (1967).
- [12] Wigner, Eugene Paul, *On the Quantum Correction for Thermodynamic Equilibrium*, Physical Reviews, **40**, 749-759 (1932)